Supplementary Information

Exactly Controlled Linear CO Liberation: A- and B-Ring Simultaneously Extended Flavonol-Based Red Fluorescent PhotoCORM

Table of Contents

Figure S5. (a) The calibration curve of the CO concentration analysis by GC analysis. (b) GC spectrum for the photo-reaction gas product CO from **Nbp-flaH**.

Figure S6. (a) Cyclic voltammograms of **Nbp-flaH** (2 mM in DMF) under N_2 (red), subsequently under air (black) at rt. (b) Absorption spectra of **Nbp-flaH** (0.4 mM in DMF) in the absence (under N_2, black) and presence of NBT (0.4 mM in DMF) under N_2 (red) and O_2 (blue) at rt.

Figure S7. Plots of the cell viability *vs*. analyte concentration. (a) **Nbp-flaH**, (b) the **Nbp-flaH** photolysis products.

Figure S8. The confocal fluorescence images of before and after the **Nbp-flaH**-treated HeLa cells were irradiated by visible light or sun light in air at rt.

Figure S9. FT−IR spectra of **Nbp-flaH**

Figure S10. ^{1}H NMR spectrum of **Nbp-flaH**.

Figure S11. ^{13}C NMR spectrum of **Nbp-flaH**.

Figure S12. HRMS spectrum of **Nbp-flaH**.

Experimental Section

Materials and Instruments.

The chemicals and reagents used in this experiment are of analytical grade or chromatographic grade and further purified by the standard method if necessary. FT-IR spectra were recorded with a Nicolet 6700 spectrophotometer. ^{1}H NMR and ^{13}C NMR spectra were recorded on a Bruker 400 WB and 500 WB, respectively (TMS as the internal standard). UV−vis spectra were measured using an Agilent Technologies HP8453 diode array spectrophotometer. The fluorescence spectra were recorded on an FL 6500 fluorescence spectrophotometer (Perkin Elmer Co., Ltd.). ESI−MS (electrospray ionization mass spectra) measurements were performed on Agilent Technologies HP1100LC-MSD. The organic reaction products analysis was performed on a Thermo Fisher Scientific LTQ Orbitrap XLHPLC−MS. The CO concentration was determined using a GC (Techcomp 7900, Shanghai Jingke). The cytotoxicity assay was accomplished using the MTT method with a microplate reader (Infinite M200 Pro). The Cell images were performed with a confocal laser scanning microscope (LEICA TCS SP5 II, Germany). Cyclic voltammetry data was collected using a CHI620b system. All CV data were obtained under N_2 in DMF with an **Nbp-flaH** concentration of 2 mM and $KClO_4$ (0.1 M) as the supporting electrolyte. The scan rate was 50 mV s^{-1}. The experimental setup consisted of a glassy carbon working electrode, a silver reference electrode, and a platinum wire auxiliary electrode. All potentials are reported *vs*. SCE.

Spectral Properties.

The stock solutions of **Nbp-flaH** (1 mM) were prepared in DMSO. For typical absorption and fluorescence spectra measurements, **Nbp-flaH** was diluted to 10 μM in DMSO-PBS buffer (1:1, V/V, 10 mM, pH 7.4). 3.0 mL of the resulting solution was placed in a 10 mm path-length quartz cell. Then the UV-vis and the fluorescence spectra in different solvents were recorded at 37 °C. The fluorescence spectra collection conditions were optimized as the excitation wavelength λ_{ex} = 405

nm, slit width: d_{ex} = d_{em} = 10 nm.

CO Photo-releasing Reaction Kinetics and Their Products Analysis

CO Photo-releasing Reaction Kinetics: The **Nbp-flaH** (10 μM in 3 mL DMSO-PBS buffer (1:1, V/V, 10 mM, pH 7.4)) solution was irradiated by visible light (intensity = 5.33×10^3 lx) under O_2 with stirring at rt. The absorption and fluorescence spectra were recorded in 1−10 min time intervals until the reaction was finished. The reaction process was monitored by the disappearance of the 420 nm absorbance or the 610 nm fluorescence intensity (accompanying the red fluorescence quenching).

Gas Product Analysis: The O_2 saturated solution of **Nbp-flaH** (the desired concentration (20−60 μM) in 1 mL ethanol) in a fixed volume flask was sealed. The solution was irradiated by visible light (intensity = 0.23−2.89 × 10^3 lx) for the desired time with stirring at rt. The photoreaction process was followed by monitoring the disappearance of the bright red fluorescence using a 365 nm UV lamp. After **Nbp-flaH** was decomposed completely, the irradiation was stopped. After finishing the visible light irradiation, the reaction solution was stirred for 12 minutes. Then the headspace gas (1 mL), including released CO, was injected into a Gas Chromatography with an FID (flame ionization detector) (CO was reduced to methane by translation stove) (5A column (TDX-01: 4 mm × 3 m, Column number: TL0686)). The GC spectra were recorded, and the concentration and yield of the released CO were calculated using the standard calibration curve.

Organic Product Analysis: After the photo-reaction in ethanol (4.5% DMF), the reaction solution was concentrated by evaporation and the remaining residue was dissolved in 5 mL of ethanol (total 0.5 mM). The reaction mixture was injected into HPLC−MS for organic products analysis with an online DAD detector (λ: 254 nm) at rt. The analysis conditions are as follows. Column: Hypersil GOLD C 18 column, Thermo Fisher Scientific 150 mm × 2.1 mm, 5 μm; Mobile phase: MeOH and HOAc-NH_4OAc buffer solution (5 mM, pH = 3) with some gradient; Flow rate: 0.5 mL min^{-1}.

Photo-release of CO in HeLa cells

Cell Culture and Cytotoxicity Assay: Cytotoxicity was investigated by the MTT [3-(4,5-dimethyl-2-thiazolyl)-2,5-diphenyl-2H-tetrazolium bromide] method. HeLa cells were seeded in a 96-well culture plate with a Dulbecco's Modified Eagle's Medium (DMEM, 10% FBS (fetal bovine serum), 100 mg/mL penicillin and 100 μg/mL streptomycin) and cultured in a 5% CO_2, humidified incubator for 24 h at 37 °C. The cells were treated in quintuplicate wells with each concentration of neat test compounds (final concentration of 1, 5, 10 and 15 μM in DMEM (DMSO = 0.2%, including a vehicle control)) and then incubated for 24 h in the dark. After removing the medium, the cells were washed 3 times with isotonic saline solution and then incubated with MTT (0.5 mg/mL in isotonic saline solution, 100 μL each well) for 4 h. After removing the medium, 200 μL DMSO was added to each well to dissolve the formazan crystals. Then the 490 nm and 750 nm (reference wavelength) absorbance were measured by a microplate reader.

The cell viability was calculated as follows:

Cell viability (%) = (average absorbance of treatment group - average absorbance of the blank group)/ (average absorbance of the control group - average absorbance of the blank group)

Imaging of the CO Photo-releasing in HeLa cells: HeLa cells were seeded in the petri dish with a DMEM medium and cultured in a 5% CO_2, humidified incubator for 24 h at 37 °C and allowed to adhere to the petri dish. To track the CO photo-releasing process of **Nbp-flaH**, HeLa cells were incubated with **Nbp-flaH** (10 μM in isotonic saline solution with 0.2% DMSO, 30 min) at 37°C. After the HeLa cells were washed with isotonic saline solution 3 times, then imaged by confocal fluorescence microscope in the red channel (λ_{ex} = 405 nm, λ_{em} = 598–618 nm). Then, the CO-releasing process of **Nbp-flaH** in HeLa cells was imaged (1.5 s interval time) and tracked in situ *via* continuous irradiation by 405 nm laser (0.83 mW, 91% laser power) in the air at rt. To demonstrate that **Nbp-flaH** can also be photo-released by visible light or sunlight in living HeLa cells, after

imaging **Nbp-flaH**-treated HeLa cells, 1 mL DMEM medium was added to HeLa cells. Then, HeLa cells were irradiated by visible light (intensity = 5.6×10^2 lx, 10 min) or sun light (17 ℃, 1 h) in the air at rt. Wash HeLa cells with isotonic saline solution three times and then image them.

Synthesis of Nbp-flaH.

Nbp-flaH was synthesized according to the following procedure (Scheme S1)[1] and characterized by FT-IR, ^{1}H NMR, ^{13}C NMR and HRMS (Figure S5− Figure S8).

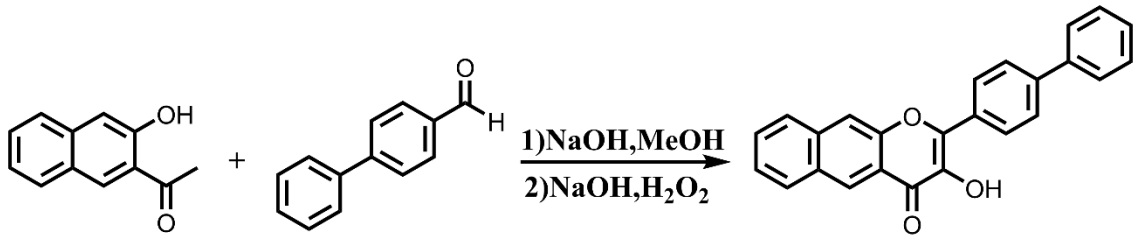

Scheme S1. The synthesis procedure of **Nbp-flaH**

The mixture of [1,1'-biphenyl]-4-carbaldehyde (0.40 g, 2.15 mmol) and sodium hydroxide (0.24 g, 6 mmol) in 100 mL anhydrous methanol was stirred and refluxed at 66℃. Then 1-(3-hydroxynaphthalen-2-yl) ethan-1-one (0.39 g, 2.15 mmol, dissolved in 2.5 mL methanol and 1.5 mL dichloromethane) was slowly added. After 4 hours of reaction, lower the reaction temperature to room temperature. Then 0.5 mL of hydrogen peroxide was slowly added dropwise at 0℃, Precipitation gradually appeared in the reaction solution, after 5 hours of reaction, a large amount of precipitation appeared, pour into crushed ice water, stir, filter with suction, wash with ice water. The obtained crude product (yellow solid) was purified by column chromatography (R_f = 0.57, dichloromethane:petroleum ether = 2:1). Finally got yellow solid pure product (0.55 g, 70 %), The molecular formula is $C_{25}H_{16}O_3$. HRMS (ESI): *m/z* (pos.): calculated for $[M + H]^+$: 365.1166, $[M + Na]^+$: 387.0986, $[2M + Na]^+$: 751.2085, Found for $[M + H]^+$: 365.1166, $[M + Na]^+$: 387.0986, [2M

+ Na]$^+$: 751.2085. ^{1}H NMR (400 MHz, DMSO–d_6): δ (ppm) = 9.73 (s, 1H), 8.86, (s, 1H), 8.42–8.40 (m, 2H), 8.35 (s, 1H), 8.27 (d, J = 4 Hz, 1H), 8.10 (d, J = 2 Hz, 1H), 7.93 (d, J = 4 Hz, 2H), 7.81 (d, J = 4 Hz, 2H), 7.69 (t, J = 6 Hz, 1H), 7.60–7.52 (m, 3H), 7.44 (t, J = 6 Hz, 1H). ^{13}C NMR (125 MHz, DMSO–d_6): δ (ppm) = 174.37, 151.37, 146.16, 141.87, 139.60, 138.44, 135.88, 130.98, 129.88, 129.56, 129.28, 128.91, 128.58, 127.68, 127.29, 127.20, 126.37, 121.39, 114.67 (19 signals expected and observed). IR: v (cm^{-1}) = 3186 (s), 1640 (s), 1597 (s), 1467 (s), 1281 (s).

Refrences

1. M. Rode, R. C. Gupta, B. K. Karale and S. S. Rindhe, *J. Heterocycl. Chem.*, 2008, **45**, 1597−1602.

Table S1. Comparison of the flavonol based photoCORMs.

Compounds	$\lambda_{abs.}$ (nm)	λ_{em} (nm)	Stokes shift (nm)	c (μM)	CO release			Reference
					λ_{ir} (nm)	t_{ir} (min)	Yield (%)	
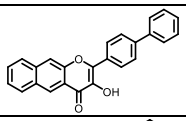	354 393 412	445 614	202	10	Visible light	13	> 90	This work
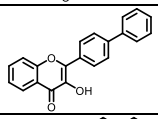	360	546	122/ 186	20	Visible light	24	> 90	*J. Mater. Chem. B* **2021**, *9*, 8263–8271.
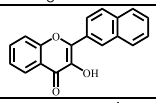	359	544	155	15	Visible light	60	82	*New J. Chem.* **2022**, *46*, 16151–16160.
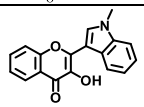	397	464	67	10	Visible light	30	> 90	*Analyst* **2022**, *147*, 3360–3369.
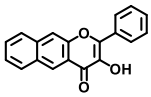	410	575	165	25	419	~8	96	*J. Am. Chem. Soc.* **2017**, *139*, 9435–9438.
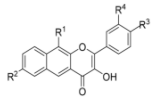	401- 455	576- 622	138 - 209	5-100	405/45 0 /460		50±4 – 95±5	*J. Org. Chem.* **2022**, *87,* 4750−4763.
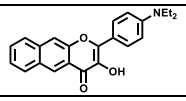	445	550	105	5	419	23	99	*ACS Med. Chem. Lett.* **2022**, *13* (2), 236–242.
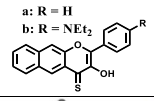	480/5 50	570/ 625	90/75	50	419, > 546	24 h	100	*ChemistryOpen* **2015**, *4,* 590−594
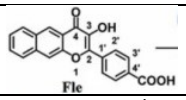	472	572	100	5	808	48 h	100	*Adv. Healthcare Mater.* **2021**, 10, 2001728
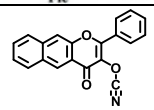	410	575	165	25	419	~8	96	*Chempluschem* **2017**, *82*, 1408–1412.
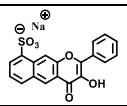	410	480 610	200	50	419		100	*J. Med. Chem.* **2019**, *62* (21), 9990–9995.
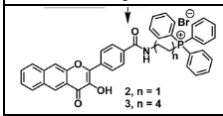	410	480 603	193	50	419	~24 h	98-100	*ACS Chem. Biol.* **2018**, *13,* 2220−2228.
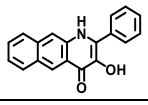	449	500 600	149	2	419	90	84	*J. Am. Chem. Soc.* **2018**, *140*, 9721–9729.
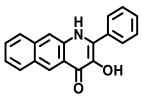	449	500 600	149	0.66 mM	419	12	90	*RSC Adv.,* **2022**, 12, 2751–2758.
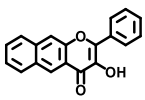	410	575	165	10	405	10	96	*Angew. Chemie - Int. Ed.* **2018**, *57*, 12415–12419.
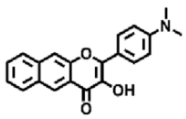	440	568	128	50 μg/mL	Xenon lamp	23	~100	*Chem. Eng. J.,* **2023**, *463*, 142371.
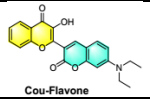	445	555	110	10	460	20	99	*Chem. Commun.* **2019**, *55*, 8987–8990.

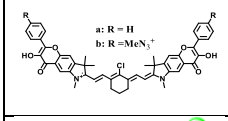	791/793	815/819	24/26	4	770/820	~180	125±15/131±6	*Chem. - A Eur. J.* **2020**, *26* (58), 13184–13190.
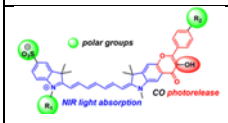	749-755	779-783	28-33	10	770	120	50±2 - 78±3	*Chem. Commun.*, **2022**, 58, 8958-8961.
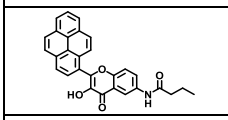	360	490	130	10	365	10	55	*Chem. Commun.* **2019**, *55*, 6301–6304.
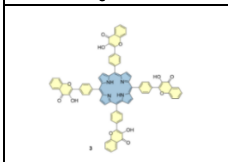	426 517 554 591 650	652 717	67	5	440	240	330	*chemRxiv* 10.26434/chemrxiv-2022-b56l1
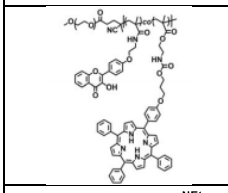	356	532	176	0.1 g/L	650 365	90	69/58	*Angew. Chemie Int. Ed.* **2021**, *60* (24), 13513–13520.
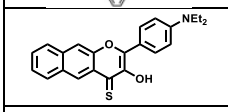	540	620 680	140	30 µg/mL	290–800	2.5	~100	*Nano Res.* 2023 s12274-023-5458-8
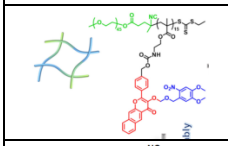	245 321	475 607	286	0.1 g/L	410	200	63.3	*Polymers.*, **2022**, *14*, 2416
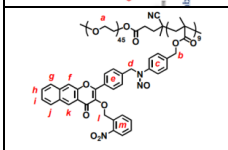	410	603	193	100µg/mL	410	120	~40	*Angew. Chem. Int. Ed.* **2022**, *61 (3),* e202112782.
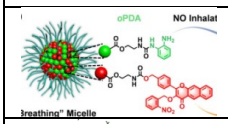	270, 334	600	266	0.1 g/L	410	40	35.1	*Angew. Chemie - Int. Ed.* **2020**, *59* (49), 21864–21869.
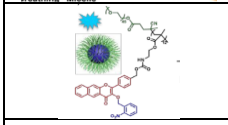	270 336 385	606	221	0.1 g/L	410	180	96	*Chem. Sci.* **2020**, *11* (17), 4499–4507.
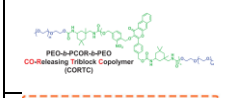	272 338 391	497 609	218	0.1 g/L	410	120	31.1	*Macromol. Rapid Commun.* **2020**, *41*, 2000323–2000331.
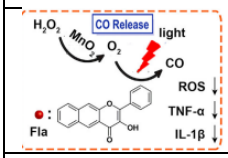	409	577	168	0.1 mM	410	8	58	*iScience* **2020**, *23* (9), 101483–101493.
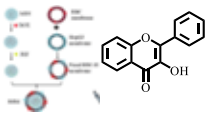	334			10 mM	980	15	93	*Chem. Commun.*, **2022,** *58,* 8512-8515.

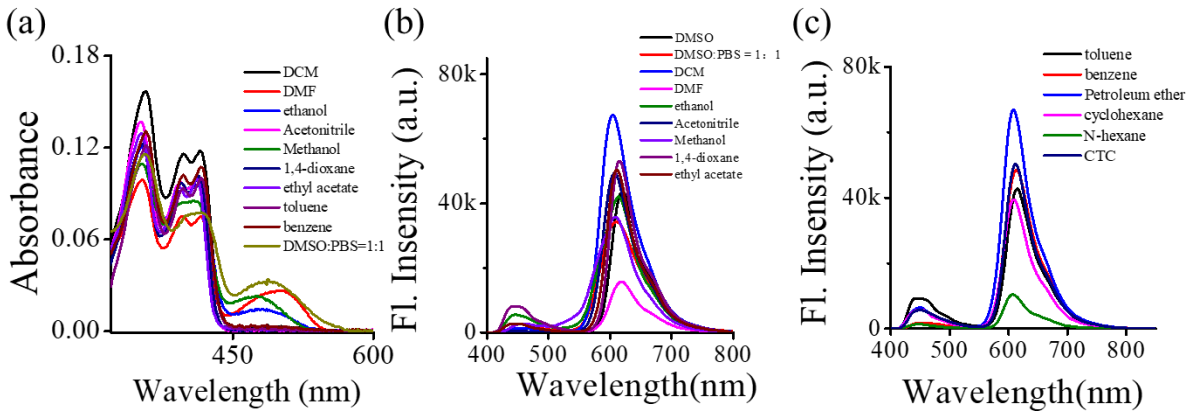

Figure S1. Spectral features of **Nbp-flaH** in various solvents (1% DMSO) at 37 ℃. (a) absorption spectra. Fluorescence spectra (b) in polar and/or protic solvents, (c) in non-polar and non-protic solvents. (10 μM, λ_{ex} = 405 nm, slit width: d_{ex}/d_{em} = 10 nm)

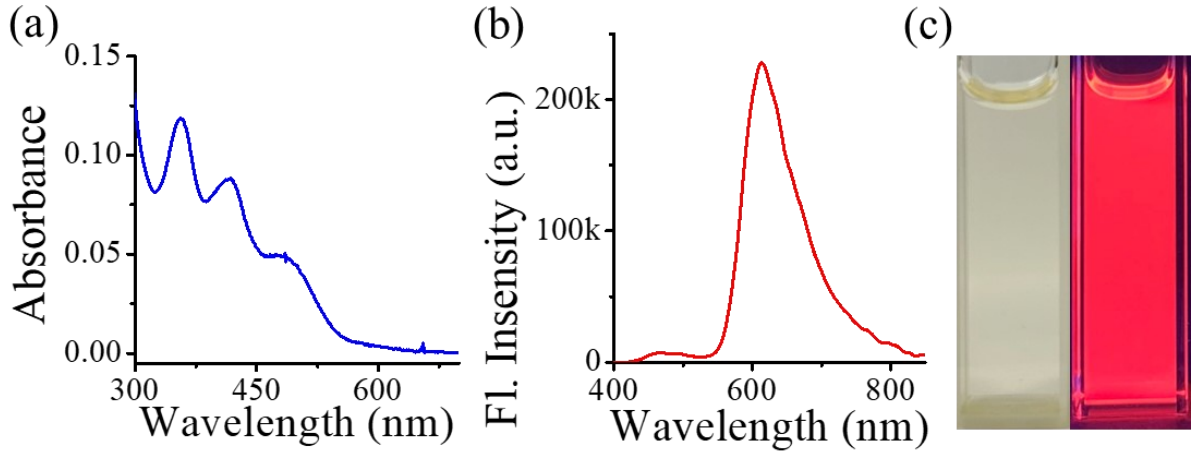

Figure S2. (a) Absorption and (b) fluorescence spectra of **Nbp-flaH**. (c) The photos of the corresponding solution color under ambient light (left) and 365 nm light (right). Conditions: 10 μM in 3 mL DMSO-PBS buffer (1:1, V/V, 10 mM, pH 7.4), λ_{ex} = 405 nm, slit width: d_{ex}/d_{em} = 10 nm.

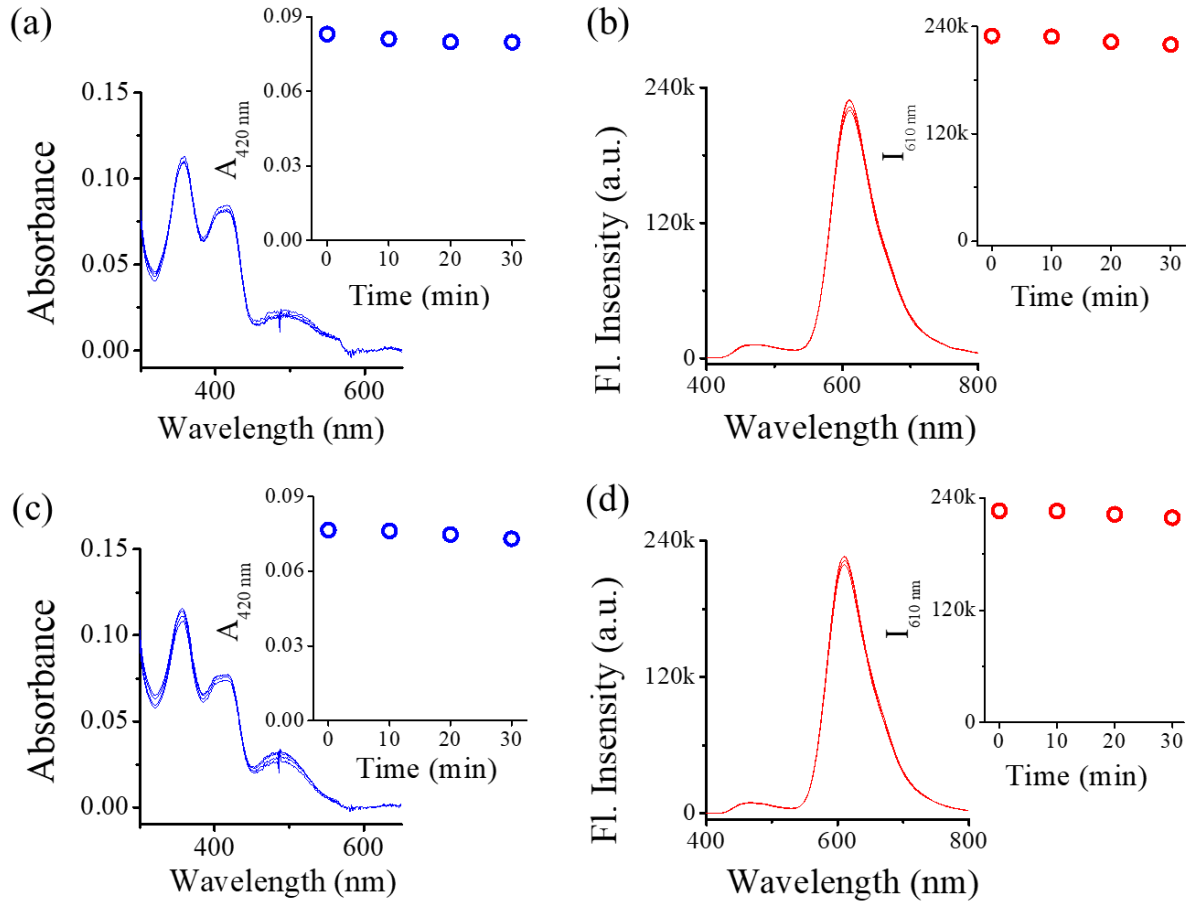

Figure S3. The time-dependent spectral change and time traces (insets) of **Nbp-flaH** under N_2 and dark. (a) absorption and (b) emission spectra under N_2; Insets: (a) $A_{420\ nm}$ and (b) $I_{610\ nm}$; (c) absorption and (d) emission spectra under dark; Insets: (c) $A_{420\ nm}$ and (d) $I_{610\ nm}$. Conditions: **Nbp-flaH** 10 μM in DMSO-PBS buffer (1:1, V/V, 10 mM, pH 7.4), λ_{ex} = 405 nm, slit width: d_{ex}/d_{em} = 10 nm.

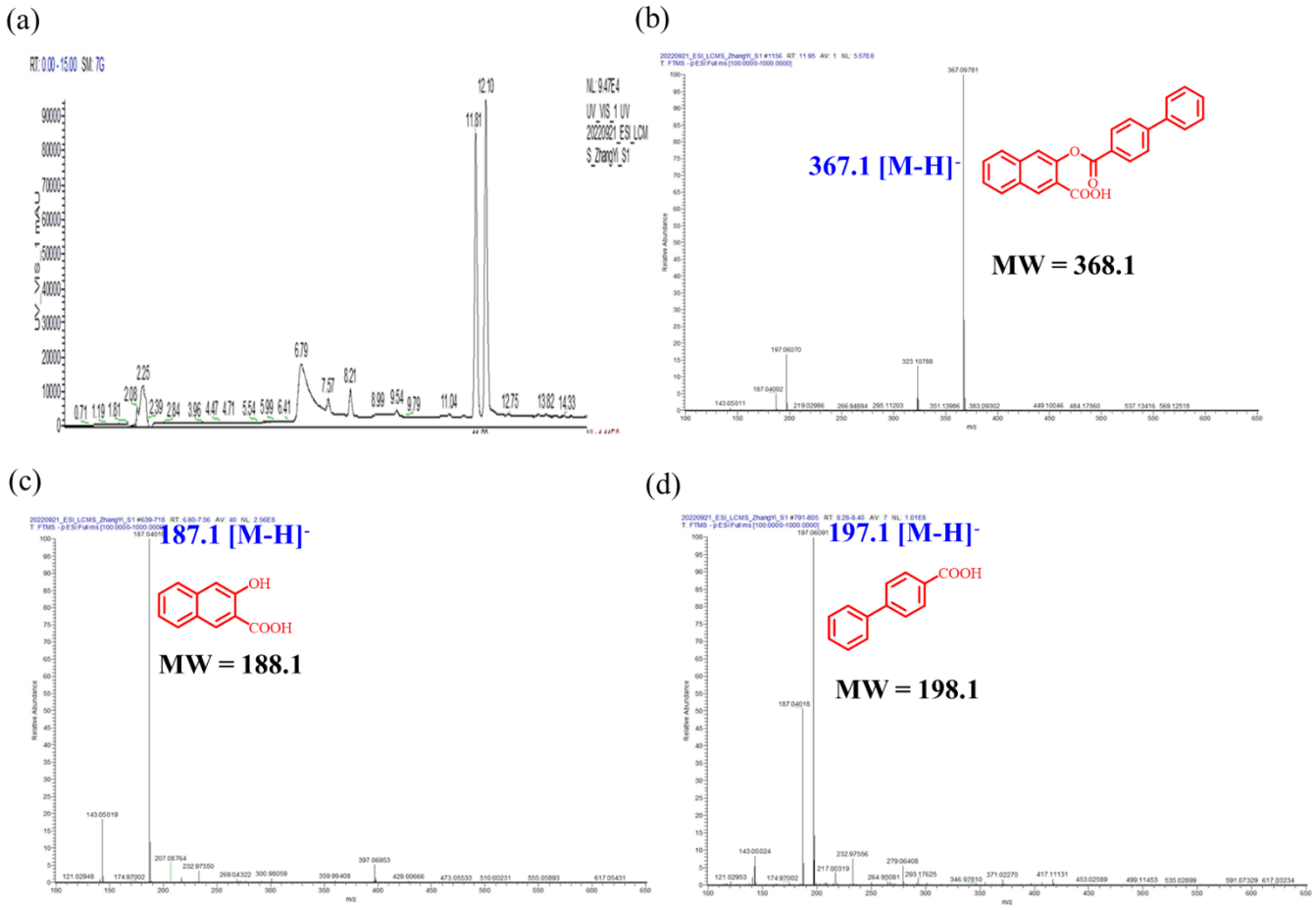

Figure S4. HPLC−MS spectra for the photo-reaction organic products from **Nbp-flaH**. (a) HPLC spectrum. MS spectra of (b) **Nbp-flaH-HObs** (*m/z* (neg.): 367.1 $(M–H)^–$), (c) 3-hydroxy-2-naphthoic acid (*m/z* (neg.): 187.1.1 $(M−H)^–$), (d) [1,1'-biphenyl]-4-carboxylic acid (*m/z* (neg.): 197.1 $(M–H)^–$).

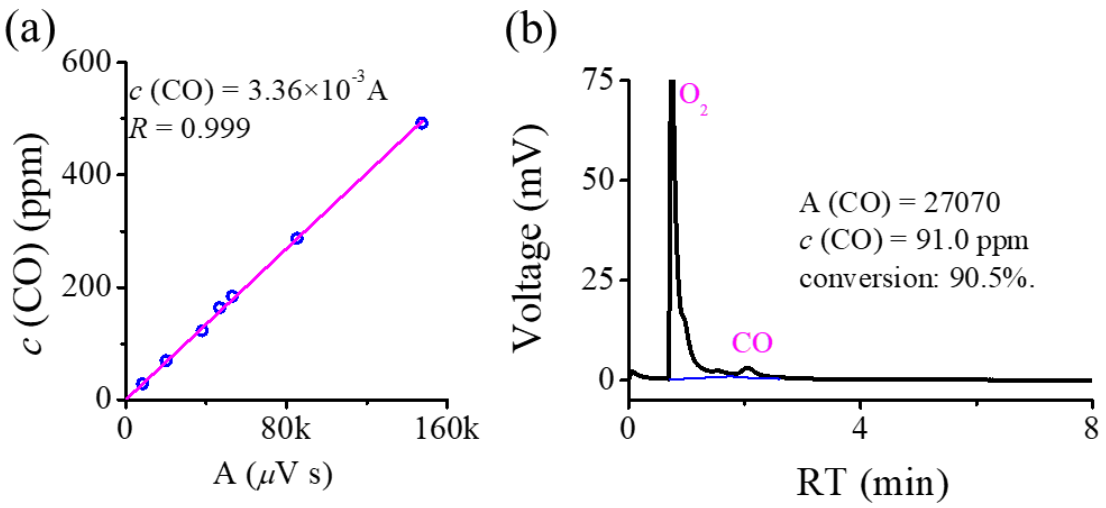

Figure S5. (a) The calibration curve of the CO concentration analysis by GC analysis. (b) GC spectrum for the photo-reaction gas product CO from **Nbp-flaH** (30 μM in ethanol with 1% DMSO) irradiated by sunlight (17℃, 3 h). "A" represents the peak area.

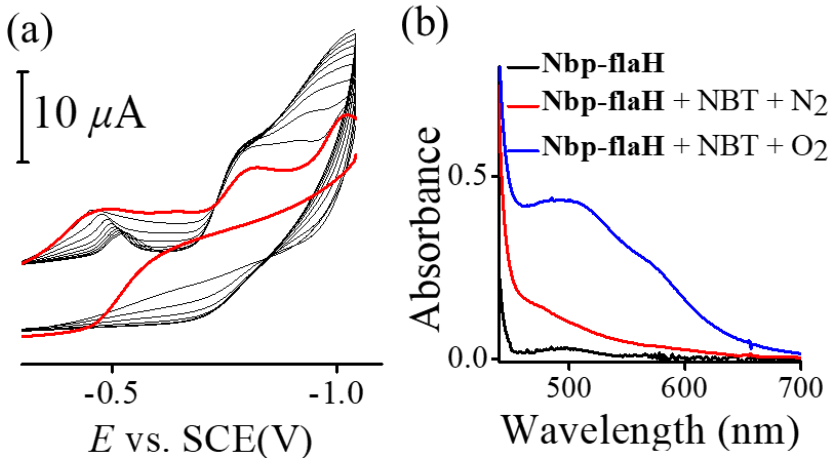

Figure S6. (a) Cyclic voltammograms of **Nbp-flaH** (2 mM in DMF) under N_2 (red), subsequently under air (black) at rt. (b) Absorption spectra of **Nbp-flaH** (0.4 mM in DMF) in the absence (under N_2, black) and presence of NBT (0.4 mM in DMF) under N_2 (red) and O_2 (blue) at rt.

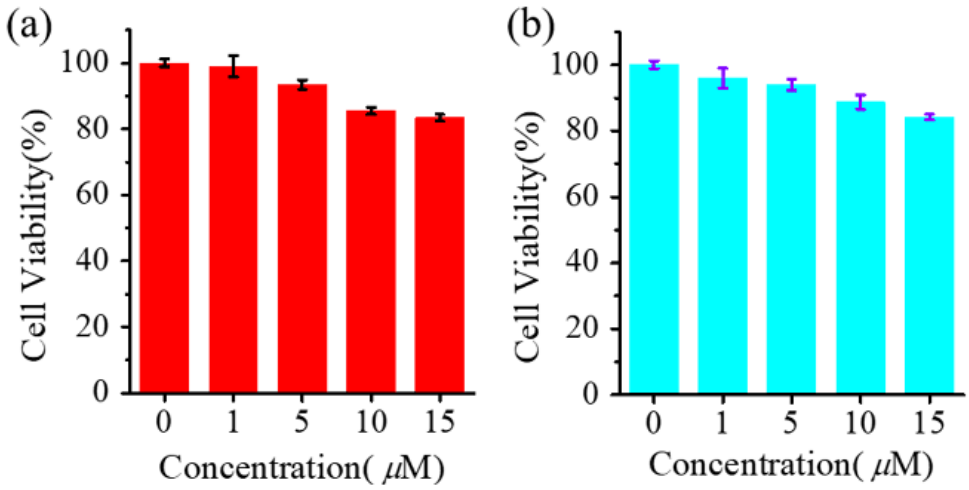

Figure S7. Plots of the cell viability *vs*. analyte concentration (a) **Nbp-flaH**, (b) the **Nbp-flaH** photolysis products (incubation time: 24 h). Error bars in column represent standard deviations of three independent measurements.

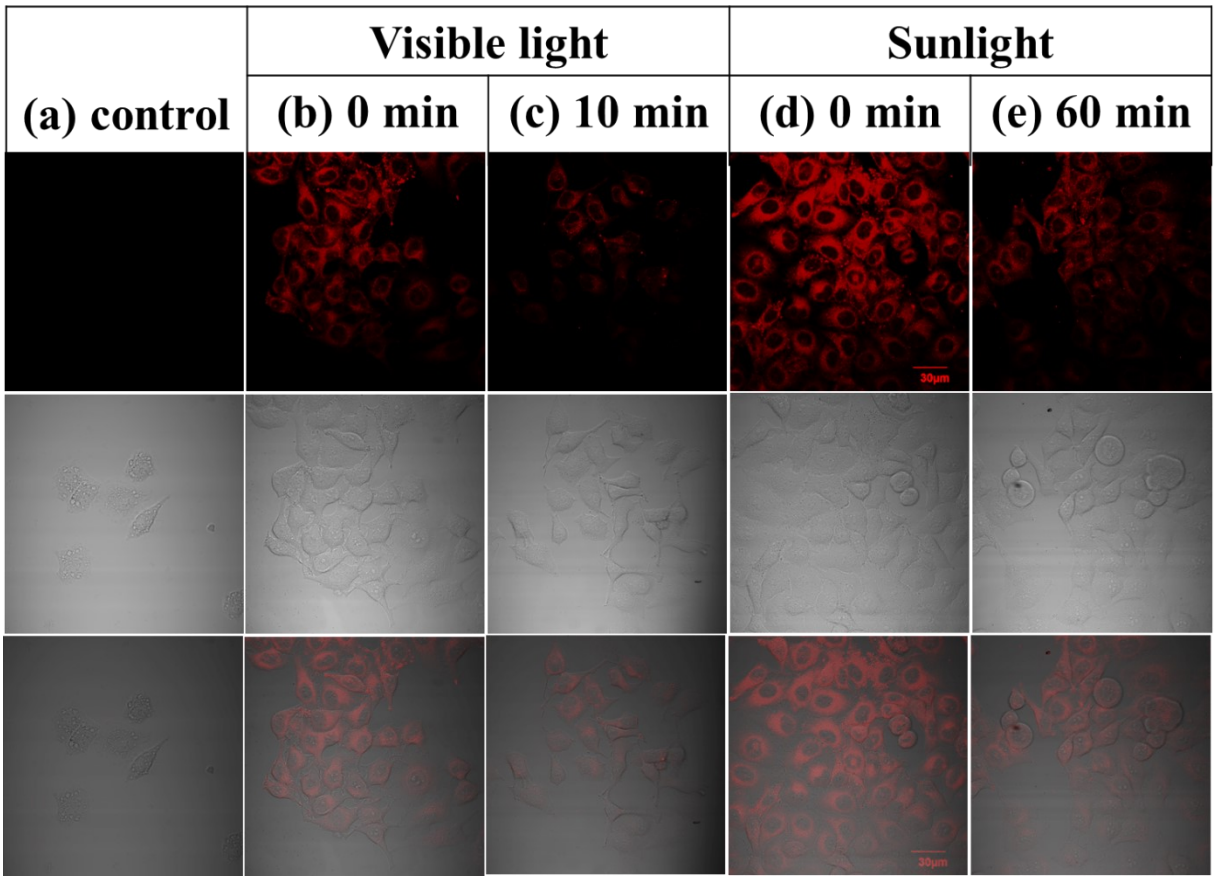

Figure S8. The confocal fluorescence images of before and after the **Nbp-flaH**-treated HeLa cells were irradiated by visible light or sun light in air at rt. (a) control, visible light (b) 0 min and (c) 10 min, sun light (d) 0 min and (e) 1 h. First row: red channel; second row: bright field; third row: merged. Conditions: 10 μM in isotonic saline solution with 0.2% DMSO, 30 min; visible light intensity = 5.6×10^2 lx; sun light: 17 ℃.

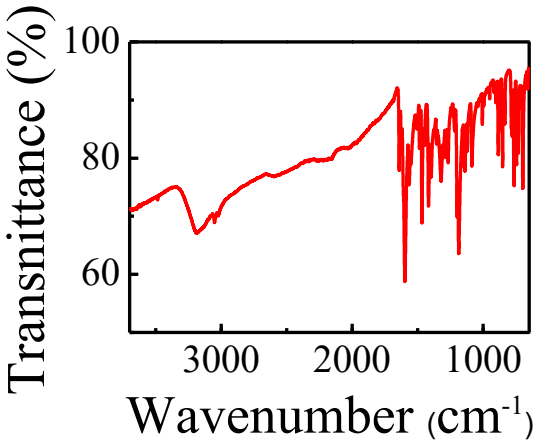

Figure S9. FT−IR spectrum of **Nbp-flaH**

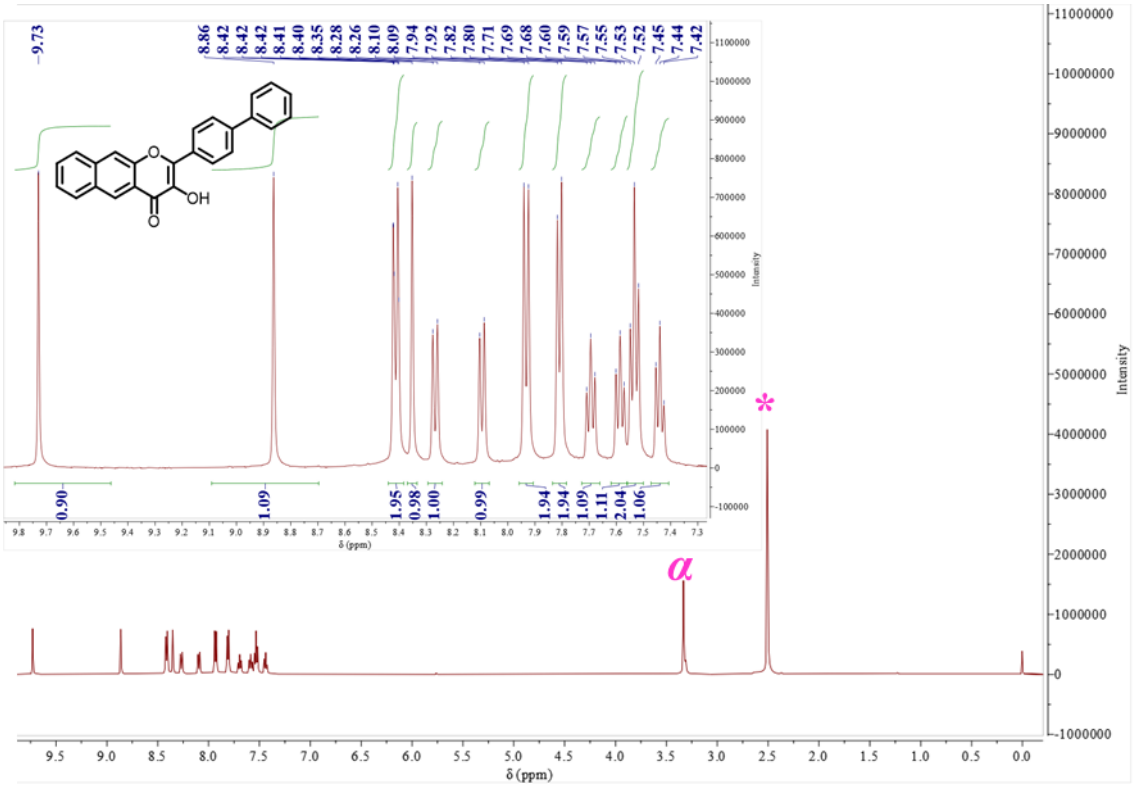

Figure S10. ^{1}H NMR (400 MHz) spectrum of **Nbp-flaH** in DMSO-d_6 at ambient temperature. The * indicates the signal from residual DMSO in the solvent. The $^{\alpha}$ indicates the signal from the residual water in the solvent.

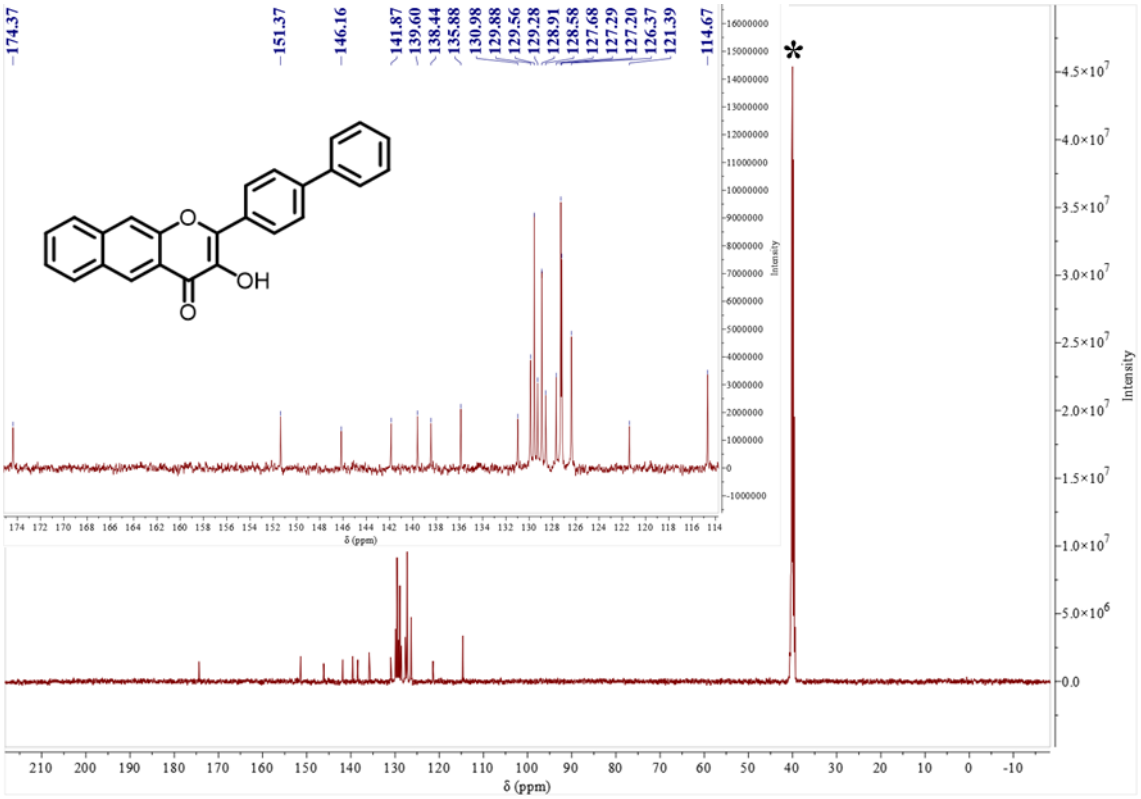

Figure S11. ^{13}C NMR (125 MHz) spectrum of **Nbp-flaH** in DMSO-d_6 at ambient temperature.

The * indicates the signal from residual DMSO in the solvent.

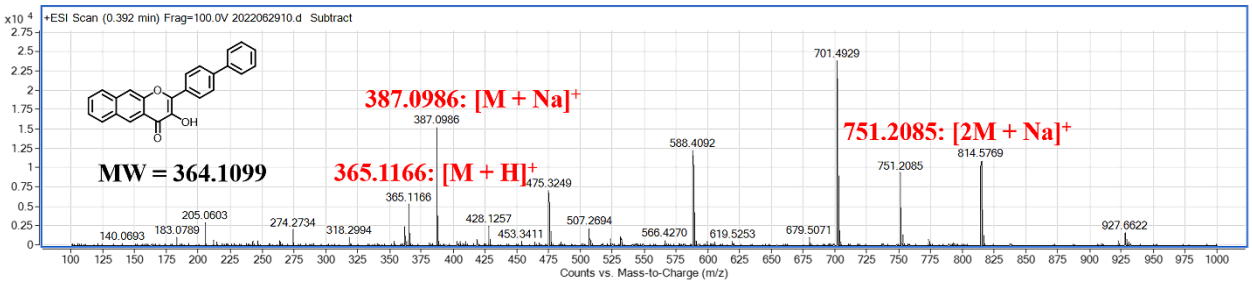

Figure S12. HRMS spectrum of **Nbp-flaH** in ethanol.